Correspondence

Joint Design of Pilot Power and Pilot Pattern for Sparse Cognitive Radio Systems

Chenhao Qi, *Member, IEEE*, Lenan Wu, Yongming Huang, *Member, IEEE*, and A. Nallanathan, *Senior Member, IEEE*

***Abstract*—Existing works design the pilot pattern for sparse channel estimation, assuming that the power of all pilots is equal. However, equal power allocation is not optimal in cognitive radio (CR) systems. In this correspondence, we jointly design the pilot power and pilot pattern for sparse channel estimation in orthogonal-frequency-division-multiplexing-based CR systems, based on the rule of mutual incoherence property that minimizes the coherence of the measurement matrix used for the sparse recovery. Under the sum power constraint and peak power constraint, the pilot design is formulated as a joint optimization problem, which is then decoupled into tractable sequential formations. Given a pilot pattern, we formulate the design of pilot power as a second-order cone programming. Then, we propose a joint design algorithm, which includes discrete optimization for pilot pattern and continuous optimization for pilot power. Simulation results show that the proposed algorithm can achieve better channel estimation performance in terms of mean square error and bit error rate and can further improve the spectrum efficiency by 2.4%, compared with existing algorithms assuming equal pilot power.**

***Index Terms*—Cognitive radio (CR), compressed sensing (CS), orthogonal frequency-division multiplexing (OFDM), pilot design, sparse channel estimation.**

I. Introduction

Radio spectrum is a precious and limited resource for wireless communications. In attempts to relieve the spectrum shortage, the concept of cognitive radio (CR) is proposed, which allows secondary users (SUs) to opportunistically access the spectrum that is originally allocated to primary users (PUs). SUs start communications with each other when the spectrum is not used by any PU. Therefore, CR can improve the usage of existing frquency bands without allocating a new spectrum resource [1]. On the other hand, with the great capability in combating frequency-selective fading and the high flexibility in allocating transmit resources, orthogonal frequency-division multiplexing (OFDM) has been suggested as a competitive candidate in CR systems [2]. In OFDM-based CR systems, the subcarriers are noncontiguous. Hence, the efficient design of pilots including pilot pattern and pilot power is crucial to the performance of channel estimation and data detection. In [3], a scheme to design pilot symbols for OFDM-based CR systems is proposed, where the pilot design assuming equal pilot power is formulated as an optimization problem that minimizes the upper bound related to the mean square error (MSE) of least squares (LS) channel estimation. In [4], a scheme that utilizes cross entropy (CE) optimization together with the analytical pilot power optimization is proposed to design pilot symbols to reduce the MSE of the LS channel estimation. In [5], parameter adaptation for wireless multicarrier-based CR systems is investigated where the CE method is demonstrated to outperform the genetic algorithm (GA) and particle swarm optimization (PSO). However, all these literatures are based on the LS channel estimation.

Recently, sparse channel estimation that exploits the inherent sparse property of wireless multipath channels and applies the compressed sensing (CS) techniques for channel estimation has been proven to improve the channel estimation performance and reduce the pilot overhead compared with the LS method [6], [7]. To further improve the performance of sparse channel estimation, one effective approach is to optimize the pilot design. In [8] and [9], it has been shown that the pilot pattern generated from the cyclic different set (CDS) is optimal and have proposed a scheme to obtain a near-optimal pilot pattern when the CDS does not exist. In [10] and [11], two pilot design schemes based on CE optimization and stochastic approximation, respectively, are proposed to minimize the MSE of sparse channel estimation using the channel data. In [12], a pilot allocation method based on the GA and a shifting mechanism is proposed for sparse channel estimation in multiple-input–multiple-output OFDM systems. In [13], a pilot design scheme for OFDM transmission over two-way relay networks is presented. In [14], sparse channel estimation is first introduced in OFDM-based CR systems. Based on the results of spectrum sensing, a scheme using constrained CE optimization is proposed to obtain an optimized pilot pattern. In particular, it is shown in [14] that sparse channel estimation can achieve 11.5% improvement in spectrum efficiency with the same channel estimation performance compared with the LS channel estimation. However, all existing works design the pilot pattern for sparse channel estimation assuming that the power of pilots is equal.

In this correspondence, based on the work of Qi et al. in [14], we further consider the pilot power optimization for sparse channel estimation in OFDM-based CR systems. Note that the CR system employing sparse channel estimation is termed as the sparse CR system in this work. We jointly design the pilot power and pilot pattern based on the rule of mutual incoherence property (MIP) that minimizes the coherence of the measurement matrix used for the sparse recovery. Under the sum power constraint and peak power constraint, the pilot design is formulated as a joint optimization problem, which is then decoupled into tractable sequential formations. Given a pilot pattern, we formulate the design of pilot power as a second-order cone programming (SOCP). Then, we propose a joint design algorithm, which includes discrete optimization for pilot pattern and continuous optimization for pilot power.

The notations used in this correspondence are defined as follows. Symbols for matrices (uppercase) and vectors (lowercase) are in boldface. $(\cdot)^T$, $(\cdot)^H$, $\mathrm{diag}\{\cdot\}$, $\boldsymbol{I}_L$, $\setminus$, $\mathbb{C}^{M\times N}$, $\mathbf{0}^{M\times N}$, $\mathcal{CN}$, $|\cdot|$, $\|\cdot\|_0$, $\|\cdot\|_2$, $\|\cdot\|_\infty$, $\mathrm{Re}\{\cdot\}$, and $\mathrm{Im}\{\cdot\}$ denote the matrix transpose, conjugate transpose (Hermitian), the diagonal matrix, the identity matrix of size L, the set exclusion, the set of $M \times N$ complex matrices, the $M \times N$ zero matrix, the complex Gaussian distribution, the absolute

Manuscript received February 27, 2014; revised July 4, 2014, and September 24, 2014; accepted November 16, 2014.This work was supported in part by the National Natural Science Foundation of China under Grants 61302097 and 61422105, by the Ph.D. Programs Foundation of the Ministry of Education of China under Grant 20120092120014, and by the Natural Science Foundation of Jiangsu Province under Grant BK20130019. The review of this paper was coordinated by Prof. X. Wang.

C. Qi, L. Wu, and Y. Huang are with the School of Information Science and Engineering, Southeast University, Nanjing 210096, China (e-mail: qch@seu.edu.cn; wuln@seu.edu.cn; huangym@seu.edu.cn).

A. Nallanathan is with the Department of Informatics, King's College London, London WC2R 2LS, U.K. (e-mail: nallanathan@ieee.org).

Color versions of one or more of the figures in this paper are available online at http://ieeexplore.ieee.org.

Digital Object Identifier 10.1109/TVT.2014.2374692

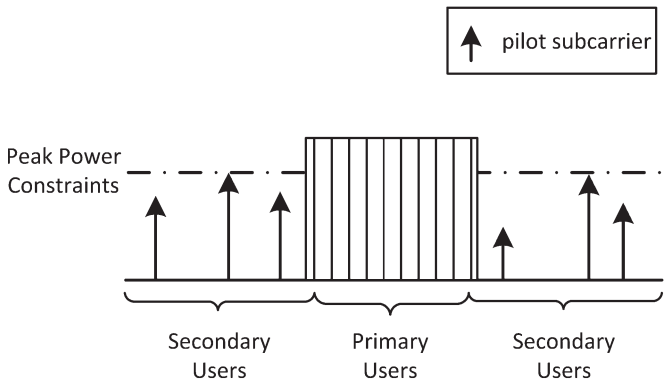

Fig. 1. Joint design of pilot power and pilot pattern for SUs under peak power constraint.

value, the ℓ_0 norm, the ℓ_2 norm, the ℓ_∞ norm, real part, and imaginary part, respectively. $\mathcal{O}(\cdot)$ denotes the order of complexity. $\hat{\phi}$ denotes the estimate of the parameter of interest ϕ.

II. Problem Formulation

We consider an OFDM-based CR system employing sparse channel estimation to exploit the inherent sparse property of wireless multipath channels. The channel is modeled as an finite impulse response filter with the channel impulse response (CIR) to be

$$\boldsymbol{h} = [h(1), h(2), \ldots, h(L)]^T. \tag{1}$$

$\boldsymbol{h}$ is sparse if the number of nonzero entries of $\boldsymbol{h}$, which is denoted as S, is much smaller than the channel length L ($S \ll L$).

Similar to [3] and [14], we assume ideal spectrum sensing without false alarm or missing detection. Based on the results of spectrum sensing, the OFDM subcarriers occupied by PUs are first deactivated. From the active subcarriers, we use some subcarriers to transmit pilot symbols and the others to transmit data symbols for SUs. We assume that the secondary transmitters of SUs broadcast the results of pilot design to the secondary receivers of SUs through control signaling.

Suppose an OFDM-based CR system with N subcarriers. After deactivating subcarriers occupied by PUs, there are $M(M \leq N)$ active subcarriers available for SUs. We denote these active subcarriers as $\mathcal{C}\{c_1, c_2, \ldots, c_M\}$, where $\mathcal{C} \subseteq \mathcal{N}$ with $\mathcal{N} = \{1, 2, \ldots, N\}$. Without loss of generality, we suppose $1 \leq c_1 < c_2 < \cdots < c_M \leq N$. From $\mathcal{C}$, we select $K(K \leq M)$ pilot subcarriers indexed by $c_{p_1}, c_{p_2}, \ldots, c_{p_K}$ $(1 \leq p_1 < p_2 < \cdots < p_K \leq M)$ to transmit pilot symbols for frequency-domain pilot-assisted channel estimation, as shown in Fig. 1. The indexes of pilot subcarriers make up a pilot pattern $\boldsymbol{p} = \{c_{p_1}, c_{p_2}, \ldots, c_{p_K}\}$, where $\boldsymbol{p} \subseteq \mathcal{C}$. We define the set of all possible pilot patterns as $\mathcal{P} \triangleq \{\boldsymbol{w} | \boldsymbol{w} \subseteq \mathcal{C},\ \|\boldsymbol{w}\|_0 = K\}$. Then, we have $\boldsymbol{p} \subset \mathcal{P}$. Note that all existing literatures of pilot design for sparse channel estimation are all based on the equal pilot power assumption. However, in OFDM-based CR systems, the pilot power can be different, as shown in Fig. 1, where the equal pilot power is not necessarily optimal. In this paper, we will study the joint design of pilot power and pilot pattern.

We denote the transmit pilot symbols and the receive pilot symbols as $\boldsymbol{x} = [x(c_{p_1}), x(c_{p_2}), \ldots, x(c_{p_K})]^T$ and $\boldsymbol{y} = [y(c_{p_1}), y(c_{p_2}), \ldots, y(c_{p_K})]^T$, respectively. For LS channel estimation, we first acquire channel frequency response (CFR) at pilot subcarriers by $\{y(i)/x(i),\ i \in \boldsymbol{p}\}$ and then make interpolations for the rest of the subcarriers. However, it usually demands a large number of pilots, i.e., $K > L$, so that the interpolations can approximate the true value of CFR. The relation between the transmit pilots and the receive pilots can be written in matrix notation as

$$\boldsymbol{y} = \boldsymbol{X}\boldsymbol{F}\boldsymbol{h} + \boldsymbol{\eta} \tag{2}$$

where

$$\boldsymbol{X} = \mathrm{diag}\left\{x\left(c_{p_1}\right), x\left(c_{p_2}\right), \ldots, x\left(c_{p_K}\right)\right\} \tag{3}$$

$$\boldsymbol{\eta} = [\eta(1), \eta(2), \ldots, \eta(K)]^T \sim \mathcal{CN}(\boldsymbol{0}, \sigma^2 \boldsymbol{I}_K) \tag{4}$$

and $\boldsymbol{F}$ is a discrete Fourier transform submatrix given by

$$\boldsymbol{F} = \frac{1}{\sqrt{N}} \begin{bmatrix} 1 & \omega^{c_{p_1}} & \cdots & \omega^{c_{p_1}(L-1)} \\ 1 & \omega^{c_{p_2}} & \cdots & \omega^{c_{p_2}(L-1)} \\ \vdots & \vdots & \ddots & \vdots \\ 1 & \omega^{c_{p_K}} & \cdots & \omega^{c_{p_K}(L-1)} \end{bmatrix}$$

where $\omega = e^{-j2\pi/N}$. We further denote

$$\boldsymbol{A} \triangleq \boldsymbol{X}\boldsymbol{F}. \tag{5}$$

Then, (2) can be written as

$$\boldsymbol{y} = \boldsymbol{A}\boldsymbol{h} + \boldsymbol{\eta}. \tag{6}$$

If $L \leq K \leq M$ and $\boldsymbol{A}$ has full column rank, (6) can be solved by LS, which essentially employs the fast Fourier transform interpolations with the estimated CIR given by

$$\hat{\boldsymbol{h}}_{\mathrm{LS}} = (\boldsymbol{A}^H \boldsymbol{A})^{-1} \boldsymbol{A}^H \boldsymbol{y}. \tag{7}$$

However, a large number of pilots is required. The CS theory shows that we can reduce the number of pilots, i.e., $2S < K < L$, by exploring the sparse property of wireless channels. To identify the positions of the S nonzero entries as well as estimating the coefficients of the S nonzero entries, which results in totally $2S$ unknown parameters, we have to use at least $K > 2S$ pilots. With this condition, we can apply CS algorithms, e.g., orthogonal matching pursuit (OMP), to estimate $\boldsymbol{h}$. Existing works have already shown that the CS algorithms outperform LS for channel estimation [15], [16].

The restrict isometry property (RIP) shows that $\boldsymbol{h}$ in (6) can be recovered from the noiseless measurement $\boldsymbol{y}(\boldsymbol{\eta} = 0)$ with a high probability if the measurement matrix $\boldsymbol{A}$ satisfies the RIP [17]. It is said that $\boldsymbol{A} \in \mathbb{C}^{K \times L}$ in (6) satisfies the RIP if there exists a constant $\delta(0 < \delta < 1)$ such that

$$(1 - \delta)\|\boldsymbol{u}\|_2^2 \leq \|\boldsymbol{A}\boldsymbol{u}\|_2^2 \leq (1 + \delta)\|\boldsymbol{u}\|_2^2 \tag{8}$$

holds for all S-sparse[1] vectors $\boldsymbol{u} \in \mathbb{C}^L$. However, it is computationally infeasible to check whether a given matrix $\boldsymbol{A}$ satisfies the RIP. Alternatively, according to [18], we can minimize the coherence of $\boldsymbol{A}$, which is known as the MIP. The MIP condition is stronger than the RIP in that the MIP implies the RIP but the converse is not true [18]. Moreover, the MIP is more intuitive and practical than the RIP. Here, we consider the pilot design including joint pilot power allocation and pilot pattern optimization with respect to the MIP.

Given a pilot pattern, i.e.,

$$\boldsymbol{p} = \{c_{p_1}, c_{p_2}, \ldots, c_{p_K}\} \tag{9}$$

and a pilot power vector, i.e.,

$$\boldsymbol{v} = \{v_1, v_2, \ldots, v_K\} \tag{10}$$

[1] $\boldsymbol{u} \in \mathbb{C}^L$ is said to be S-sparse ($S \ll L$) if the number of nonzero entries of $\boldsymbol{u}$ is equal to S or smaller than S.

with v_i denoting the power of the ith pilot symbol transmitted by the c_{p_i}th subcarrier, i.e.,

$$v_i \triangleq |x(c_{p_i})|^2, \quad i = 1, 2, \ldots, K \tag{11}$$

we define the coherence of $\boldsymbol{A}$ as the maximum absolute correlation between any two different columns of $\boldsymbol{A}$, i.e.,

$$\begin{aligned} g(\boldsymbol{p}, \boldsymbol{v}) &\triangleq \max_{0 \le m < n \le L-1} |\langle A(m), A(n) \rangle| \\ &= \max_{0 \le m < n \le L-1} \left| \sum_{i=1}^{K} v_i \omega^{c_{p_i}(n-m)} \right| \Big/ \sum_{i=1}^{K} v_i \end{aligned} \tag{12}$$

where $\langle A(m), A(n) \rangle$ denotes the normalized inner product between the mth column $A(m)$ and the nth column $A(n)$ of $\boldsymbol{A}$, i.e.,

$$\langle A(m), A(n) \rangle \triangleq \frac{A^H(m) A(n)}{\|A(m)\|_2 \|A(n)\|_2}. \tag{13}$$

Let $d = n - m$ and $\Lambda = \{1, 2, \ldots, L-1\}$. Then, (12) can be rewritten as

$$g(\boldsymbol{p}, \boldsymbol{v}) = \max_{d \in \Lambda} \left| \sum_{i=1}^{K} v_i \omega^{c_{p_i} d} \right| \Big/ \sum_{i=1}^{K} v_i. \tag{14}$$

According to the MIP, the objective for the pilot design is to minimize the coherence of $\boldsymbol{A}$, i.e., $\min_{\boldsymbol{p}, \boldsymbol{v}} \ g(\boldsymbol{p}, \boldsymbol{v})$. The constraint for the integer vector $\boldsymbol{p}$ is $\boldsymbol{p} \subset \mathcal{P}$. Suppose the sum power of all pilot symbols is

$$\sum_{i=1}^{K} v_i = V_T \tag{15}$$

where V_T is the prespecified sum power constraint of SUs. Obviously, (15) is more general in practical OFDM-based CR systems than simply assuming

$$v_1 = v_2 = \cdots = v_K = \frac{V_T}{K} \tag{16}$$

in current literatures [8]–[10]. On the other hand, SUs should properly control the peak power of pilot subcarriers regarding the linear region of power amplifiers. The power of pilot subcarriers cannot be too large or too small. As shown in Fig. 1, we denote V_H as the peak power constraint related to the saturation power of the power amplifier. Moreover, the pilot power should be greater than a threshold V_L, which is related to the cutoff power of the power amplifier as well as the noise and interference level around SUs. In particular, $V_L = 0$ can be regarded as a special case. Hence, we have

$$V_L \le v_i \le V_H, \quad i = 1, 2, \ldots, K. \tag{17}$$

With these constraints, the pilot design in OFDM-based CR systems can be formulated as

$$\begin{aligned} \min_{\boldsymbol{p}, \boldsymbol{v}} \quad & g(\boldsymbol{p}, \boldsymbol{v}) \\ \text{s.t.} \quad & \boldsymbol{p} \subset \mathcal{P} \\ & \sum_{i=1}^{K} v_i = V_T, \ V_L \le v_i \le V_H \end{aligned} \tag{18}$$

which involves the joint optimization of the discrete integer vector $\boldsymbol{p}$ and the continuous real-valued positive vector $\boldsymbol{v}$. Note that unlike most literatures, investigating the optimal power allocation to maximize the achievable rate of CR systems, in this paper, we focus on the pilot design for sparse channel estimation, where the design of data subcarriers is out of the scope of this work.

Apparently, it is analytically intractable to get a solution from (18). We now decouple this joint optimization problem with the following two kinds of sequential formulations.

1) Given a $\tilde{\boldsymbol{p}} \subset \mathcal{P}$, we first get

$$\begin{aligned} & g_v(\tilde{\boldsymbol{p}}) \triangleq \min_{\boldsymbol{v}} g(\tilde{\boldsymbol{p}}, \boldsymbol{v}) \\ & \text{s.t.} \quad \sum_{i=1}^{K} v_i = V_T, \ V_L \le v_i \le V_H \end{aligned} \tag{19}$$

then we solve

$$\min_{\tilde{\boldsymbol{p}} \subset \mathcal{P}} g_v(\tilde{\boldsymbol{p}}) \tag{20}$$

to get an optimal $\boldsymbol{p}$. Meanwhile, the corresponding $\boldsymbol{v}$ is also obtained.

2) Given a feasible $\tilde{\boldsymbol{v}}$, we first get

$$g_p(\tilde{\boldsymbol{v}}) \triangleq \min_{\boldsymbol{p} \subset \mathcal{P}} g(\boldsymbol{p}, \tilde{\boldsymbol{v}}) \tag{21}$$

then we solve

$$\begin{aligned} \min_{\tilde{\boldsymbol{v}}} \quad & g_p(\tilde{\boldsymbol{v}}) \\ \text{s.t.} \quad & \sum_{i=1}^{K} \tilde{v}_i = V_T, \ V_L \le \tilde{v}_i \le V_H \end{aligned} \tag{22}$$

to get an optimal $\boldsymbol{v}$. Meanwhile, the corresponding $\boldsymbol{p}$ is also obtained.

Comparing $\boldsymbol{p} \subset \mathcal{P}$ with the constraints in (15) and (17), it can be seen that $\boldsymbol{p}$ is less difficult to enumerate than $\boldsymbol{v}$. Therefore, it is better to decouple the joint optimization problem described by (18) with the first kind of formulations described by (19) and (20).

III. Pilot Power Allocation

Regarding (19), with a given pilot pattern $\tilde{\boldsymbol{p}} \subset \mathcal{P}$, we first generate a table, i.e.,

$$\boldsymbol{G} = \begin{bmatrix} \omega^{c_1} & \omega^{c_2} & \cdots & \omega^{c_M} \\ \omega^{2c_1} & \omega^{2c_2} & \cdots & \omega^{2c_M} \\ \vdots & \vdots & \ddots & \vdots \\ \omega^{(L-1)c_1} & \omega^{(L-1)c_2} & \cdots & \omega^{(L-1)c_M} \end{bmatrix} \tag{23}$$

where $\omega = e^{-j2\pi/N}$. Once N, L and $\mathcal{C}$ are given, $\boldsymbol{G}$ is determined.

We look up $\boldsymbol{G}$ and select the corresponding K columns indexed by $\tilde{\boldsymbol{p}}$ from $\boldsymbol{G}$, making up a $L-1$ by K submatrix $\boldsymbol{G}(\tilde{\boldsymbol{p}})$. Then, from (14), we have

$$g(\tilde{\boldsymbol{p}}, \boldsymbol{v}) = \frac{1}{V_T} \|\boldsymbol{G}(\tilde{\boldsymbol{p}}) \boldsymbol{v}\|_\infty. \tag{24}$$

Therefore, (19) is equivalent to

$$\begin{aligned} \min_{\boldsymbol{v}} \quad & \|\boldsymbol{G}(\tilde{\boldsymbol{p}}) \boldsymbol{v}\|_\infty \\ \text{s.t.} \quad & \sum_{i=1}^{K} v_i = V_T, \ V_L \le v_i \le V_H \end{aligned} \tag{25}$$

where $\tilde{\boldsymbol{p}}$ is given, and $\boldsymbol{G}(\tilde{\boldsymbol{p}})$ is a complex-valued submatrix fast generated by looking up $\boldsymbol{G}$. Let $\boldsymbol{b}_i$ denote the ith row of $\boldsymbol{G}(\tilde{\boldsymbol{p}})$, $i = 1, 2, \ldots, L-1$. We further denote

$$\boldsymbol{B}_i = \begin{bmatrix} \mathrm{Re}\{\boldsymbol{b}_i\} \\ \mathrm{Im}\{\boldsymbol{b}_i\} \end{bmatrix},\ i = 1, 2, \ldots, L-1 \tag{26}$$

which is a real-valued matrix with two rows and K columns. Then, (25) can be converted into a real-valued optimization problem as

$$\begin{aligned} \min_{z}\ & z \\ \text{s.t.}\quad & \|\boldsymbol{B}_i \boldsymbol{v}\|_2 \le z,\ i = 1, 2, \ldots, L-1 \\ & \sum_{i=1}^{K} v_i = V_T,\ V_L \le v_i \le V_H \end{aligned} \tag{27}$$

which is an SOCP optimization problem that contains $L-1$ second-order conic constraints and some linear constraints. Typically, it can be solved by SOCP solvers, e.g., MOSEK. Then, we can obtain feasible solutions as $\tilde{z}$ and $\tilde{\boldsymbol{v}}$ from (27), where $g_v(\tilde{\boldsymbol{p}}) = \tilde{z}$.

IV. Joint Pilot Design

If M and K are not small enough, $\mathcal{P}$ can be a huge set. For example, if $M = 512$ and $K = 16$, $\|\mathcal{P}\|_0 = \binom{512}{16} = 8.4 \times 10^{29}$. It is impossible for SUs to store $\mathcal{P}$ into the memory and check them one by one until the best $\boldsymbol{p} \subset \mathcal{P}$ is found. Furthermore, it is very computationally inefficient to implement the exhaustive search from such huge space, particularly for SUs equipped with power-constrained mobile devices.

The proposed joint design algorithm including discrete optimization for pilot pattern and continuous optimization for pilot power is described in Algorithm 1. At first, we input system parameters $\mathcal{C}$, N, M, K, L, J, T_1, and T_2, where T_1 and T_2 represent the number of outer-loop and inner-loop iterations, respectively. Each outer-loop iteration includes T_2 inner-loop iterations. Then, we initialize a zero-matrix $\boldsymbol{D}$ to store the results of optimized pilot patterns after running inner-loop iterations. Each row of $\boldsymbol{D}$ stores a pilot pattern $\boldsymbol{p}$, with the corresponding objective value $g_v(\boldsymbol{p})$ stored in $\boldsymbol{r}$, which is initialized to be a zero vector. Then, we generate a table $\boldsymbol{G}$ according to (23). At each outer-loop iteration, indicated from step 4 to step 16, we start by randomly generating a pilot pattern $\boldsymbol{p} \subset \mathcal{P}$. By introducing the randomness to the algorithm so that it starts from different initial pilot patterns, we can avoid that the algorithm falls into local optimums. As T_1 increases to infinity, the algorithm will converge to the global optimum. Then, we use the inner-loop iterations from step 6 to step 14 to obtain an optimized pilot pattern $\boldsymbol{p}$, which is stored in each row of $\boldsymbol{D}$ with the corresponding objective value $g_v(\boldsymbol{p})$ stored in $\boldsymbol{r}$, indicated by step 15. After we finish the outer-loop iterations, we select the minimum from $\boldsymbol{r}$ and output the corresponding row of $\boldsymbol{D}$ as the designed pilot pattern $\boldsymbol{p}_o$, indicated by step 17 and step 18. We then substitute $\boldsymbol{p}_o$ into (27) to design the pilot power.

Algorithm 1 Joint Design of Pilot Power and Pilot Pattern

1: Input: $\mathcal{C}$, N, M, K, L, J, T_1, T_2.
2: Initializations: $\boldsymbol{D} \Leftarrow \boldsymbol{0}^{T_1 \times K}$. $\boldsymbol{r} \Leftarrow \boldsymbol{0}^{T_1}$.
3: Generate $\boldsymbol{G}$ according to (23).
4: **for** $l = 1, 2, \ldots, T_1$
5: randomly generate $\boldsymbol{p} \subset \mathcal{P}$. $\boldsymbol{p}^* \Leftarrow \boldsymbol{0}^K$.
6: **for** $n = 1, 2, \ldots, T_2$
7: **if** $\boldsymbol{p} = \boldsymbol{p}^*$
8: break.
9: **end if**
10: $\boldsymbol{p}^* \Leftarrow \boldsymbol{p}$.
11: **for** $k = 1, 2, \ldots, K/J$
12: Obtain $\hat{\boldsymbol{p}}_{\boldsymbol{p},k}$ according to (31). $\boldsymbol{p} \Leftarrow \hat{\boldsymbol{p}}_{\boldsymbol{p},k}$.
13: **end for**(k)
14: **end for**(n)
15: $D(l) \Leftarrow \boldsymbol{p}$. $r(l) \Leftarrow g_v(\boldsymbol{p})$.
16: **end for**(l)
17: $t = \arg\min_{i=1,2,\ldots,T_1} r(i)$.
18: Output $\boldsymbol{p}_o = D(t)$ as the designed pilot pattern.
19: Substitute $\boldsymbol{p}_o$ into (27) to design the pilot power.

Here, we use an auxiliary vector $\boldsymbol{p}^*$, which always records the pilot pattern obtained from the previous inner-loop iteration. If we find that $\boldsymbol{p}$ is exactly the same as $\boldsymbol{p}^*$, which means we did not get a new pilot pattern, there is no need to continue the inner-loop iterations because the results thereafter will be exactly the same. Then, we break from the inner-loop iterations. These procedures are indicated from step 7 to step 10. Additionally, we have to reset $\boldsymbol{p}^*$ by $\boldsymbol{p}^* \Leftarrow \boldsymbol{0}^K$ at the start of each outer-loop iteration. This way, we can save the CPU running time and therefore improve the efficiency by skipping the same routine.

The main contribution of Algorithm 1 is the group update of entries of $\boldsymbol{p}$, which is shown from step 11 to step 13. The update of $\boldsymbol{p}$ is implemented in a group of J entries each time, where K is divisible by J, i.e., K/J is a positive integer. For $k = 1, 2, \ldots, K/J$, given the latest $\boldsymbol{p}$ from the last inner-loop iteration, we update the kth group of entries of $\boldsymbol{p}$ with the best group selected from

$$\mathcal{W} = \{\boldsymbol{w} | \boldsymbol{w} \subseteq \Psi,\ \|\boldsymbol{w}\|_0 = J\} \tag{28}$$

where

$$\Psi = \mathcal{C} \setminus \{p(i) | i = 1, 2, \ldots, K, i \notin \Phi\} \tag{29}$$

$$\Phi = \{kJ - J + 1, kJ - J + 2, \ldots, kJ\}. \tag{30}$$

Mathematically, the resultant pilot pattern $\hat{\boldsymbol{p}}_{\boldsymbol{p},k}$ with the update of the kth group of entries is given by

$$\hat{\boldsymbol{p}}_{\boldsymbol{p},k} = \arg \min_{\substack{\tilde{\boldsymbol{p}} \\ \tilde{p}(i) = p(i),\ i = 1,2,\ldots,K, i \notin \Phi \\ \{\tilde{p}(i), i \in \Phi\} \subset \mathcal{W}}} g_v(\tilde{\boldsymbol{p}}) \tag{31}$$

where the computation of $g_v(\tilde{\boldsymbol{p}})$ is provided in Section III. After we obtain $\hat{\boldsymbol{p}}_{\boldsymbol{p},k}$ for given $\boldsymbol{p}$ and k, we update $\boldsymbol{p}$ by $\boldsymbol{p} \Leftarrow \hat{\boldsymbol{p}}_{\boldsymbol{p},k}$.

The complexity for pilot power allocation given a pilot pattern in (27) is $\mathcal{O}((L-1)^{1.5}(K+1)^3)$. Therefore, the computational complexity for Algorithm 1 is

$$\mathcal{O}\left(T_1 T_2 (L-1)^{1.5} (K+1)^3 \frac{K}{J} \binom{M-K+J}{J}\right) \tag{32}$$

suppose that T_2 is small enough [19]. If T_2 is large, the inner-loop iterations will terminate itself by procedures from step 7 to step 9, leading to even lower complexity than (32).

Remark: If we set $J = K$, Algorithm 1 degenerates to be the exhaustive search, where $\|\mathcal{W}\|_0 = \binom{M}{K}$, and $\|\Phi\|_0 = K$. In this case, no matter what T_1 and T_2 are, they are equivalent to $T_1 = T_2 = 1$, resulting in $\mathcal{O}(\binom{M-K+J}{J})$, which is the extraordinarily high complexity of the exhaustive search. In practice, we usually set $J = 1$ or $J = 2$ to reduce the complexity. For example, if $J = 1$, (32) reduces to a polynomial complexity, i.e., $\mathcal{O}(T_1 T_2 (L-1)^{1.5}(K+1)^3 K(M-K+1))$.

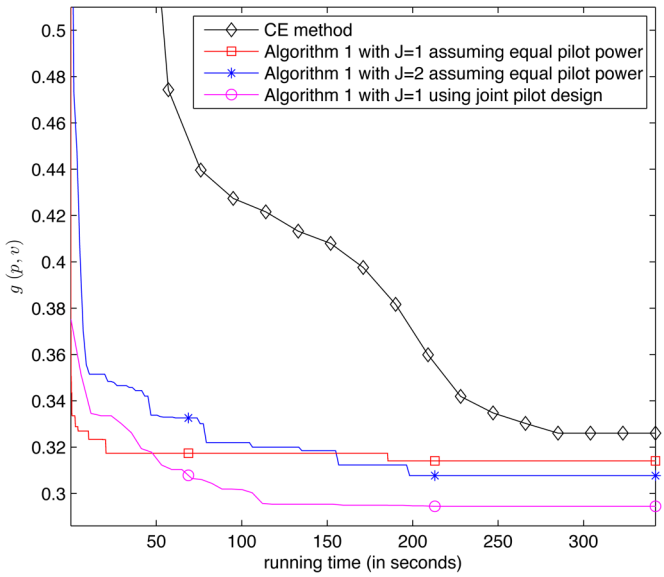

Fig. 2. Comparisons of convergence and complexity for different algorithms or parameters.

V. Simulation Results

To compare this work with [14], we set the same system parameters as [14]. We consider an OFDM-based CR system with $N = 1024$ subcarriers. After ideal spectrum sensing, there are $M = 512$ active subcarriers available for SUs, including three subcarrier blocks, i.e., $\mathcal{B}_1 = \{1, 2, 3, \ldots, 256\}$, $\mathcal{B}_2 = \{513, 514, \ldots, 640\}$, $\mathcal{B}_3 = \{897, 898, \ldots, 1024\}$, with the number of contiguous subcarriers of each block being 256, 128, and 128, respectively. From $\mathcal{C} = \mathcal{B}_1 \cup \mathcal{B}_2 \cup \mathcal{B}_3$, which can also be regarded as the union of several active CR subbands for SUs, we want to select $K = 16$ pilot subcarriers for frequency-domain pilot-assisted channel estimation. A sparse multipath channel $\boldsymbol{h}$ is generated with $L = 60$ taps, where $S = 5$ dominant nonzero channel taps are randomly placed among L taps. The channel gain of each path is independent and identically distributed complex Gaussian distributed with unit variance, i.e., $\mathcal{CN}(0, 1)$. Quaternary phase-shift keying modulation is employed in the simulations.

To evaluate the performance of Algorithm 1, we first compare it with the CE method [14] assuming equal pilot power indicated by (16), where the joint pilot design is simplified to be the pilot pattern design. We set $V_T = 1$, which means that the sum power of pilot subcarriers is normalized. We set $V_L = 0.03$ and $V_H = 0.1$ so that the pilot power does not vary too much. The steps for optimal pilot power allocation in Algorithm 1 are skipped by directly substituting $v_1 = v_2 = \cdots = v_{16} = 0.0625$ into (24). The parameters of the CE method are selected to be the best in [14], where the maximum number of iterations, the number of random samples, the sample quantile, and the smoothing factor are set to be 50, 100 000, 0.001, and 0.3, respectively. It can be seen in Fig. 2 that Algorithm 1 is much faster convergent than the CE method. Here, we compare the convergence speed with respect to the running time instead of the number of iterations, because the running time of each iteration is different for different algorithms or parameters. Since we run the simulations under the exact same computer hardware and software, the running time is proportional to the computational complexity. We set $T_1 = 1000$ and $T_2 = 15$ for Algorithm 1. Once the running time, i.e., 342 s, which is the running time for the CE method [14], is reached, we terminate Algorithm 1 so that we can compare Algorithm 1 with the CE method under the same computational complexity. As shown in Fig. 2, Algorithm 1 with $J = 1$ can achieve the best performance of the CE method in no more than 10 s, which indicates that Algorithm 1 is 34 times faster than the CE method and, therefore, is much more efficient and powerful. Since it has already been demonstrated in [5] that the CE method outperforms GA and PSO, Algorithm 1 is a remarkable candidate for integer optimization with its applications not restricted to the pilot design. As shown in Fig. 2, although Algorithm 1 with $J = 2$ converges slower than that with $J = 1$, it can achieve better performance than that with $J = 1$ if the running time is long enough, i.e., longer than 55 s. For those SUs equipped with powerful CPU and large capacity of battery, it is better to set $J = 2$ or even larger. The finally obtained pilot patterns $\boldsymbol{p}$ with the corresponding objective $g(\boldsymbol{p}, \boldsymbol{v})$ during 342 s of running time assuming equal pilot power are listed in Table I. Note that in [14], we suppose $v_1 = v_2 = \cdots = v_{16} = 1$, whereas in this paper, we suppose $v_1 = v_2 = \cdots = v_{16} = 0.0625$ satisfying $\sum_{i=1}^{16} v_i = 1$, the objective in [14] has to be divided by $K = 16$ when compared with this work.

TABLE I
Comparisons of Pilot Patterns Using Different Algorithms or Parameters

Type	$g(\boldsymbol{p}, \boldsymbol{v})$	$\boldsymbol{p}$
CE method	0.3260	47, 95, 110, 162, 180, 193, 246, 513 524, 627, 640, 897, 910, 939, 976, 1019
Algorithm 1 with $J = 1$, equal	0.3141	18, 45, 57, 103, 141, 187, 242, 256 513, 593, 609, 640, 897, 909, 926, 977
Algorithm 1 with $J = 2$, equal	0.3077	30, 46, 77, 121, 182, 228, 247, 256 513, 529, 619, 633, 905, 932, 960, 1021
Algorithm 1 with $J = 1$, joint	0.2945	1,34, 47, 98, 109, 181, 221, 236 252, 513, 529, 609, 635, 900, 934, 959

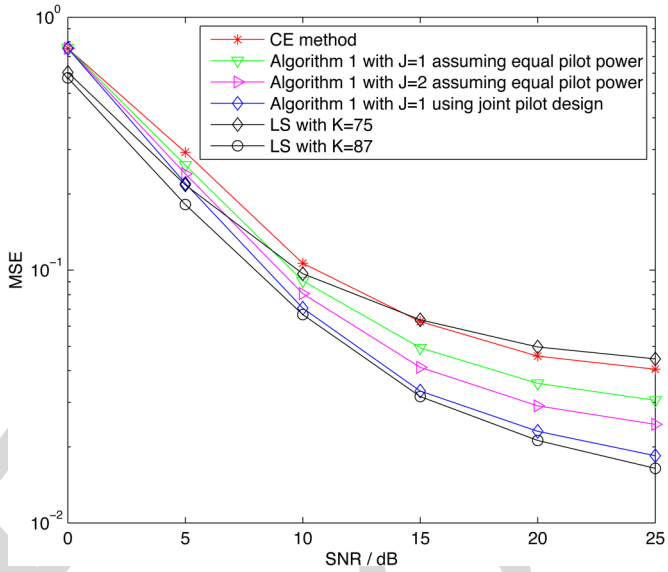

Fig. 3. Comparisons of MSE performance for different algorithms parameters.

We now evaluate the performance of joint design of pilot power and pilot pattern and compare it with the pilot design assuming equal pilot power. As shown in Fig. 2, Algorithm 1 with $J = 1$ using joint pilot design achieves better performance than Algorithm 1 with $J = 1$ or $J = 2$, while its computational complexity is between $J = 1$ and $J = 2$. The obtained pilot pattern with the corresponding objective is also listed in Table I. The comparisons of MSE performance and the bit error rate (BER) performance for sparse channel estimation are shown in Figs. 3 and 4, respectively. Both the MSE and BER are averaged

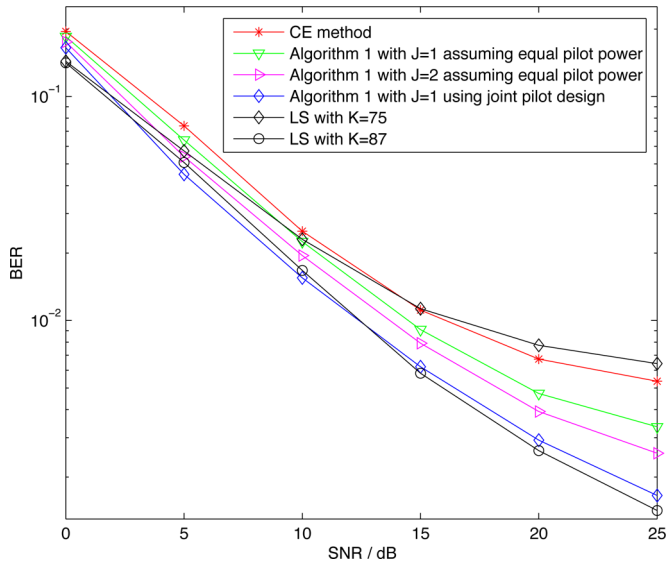

Fig. 4. Comparisons of BER performance for different algorithms or parameters.

over 10 000 sparse channel realizations. The popular OMP algorithm is employed for sparse channel estimation given the designed pilot pattern and pilot power. For comparisons, the performance of LS channel estimation using $K = 75$ and $K = 87$ equally spaced pilots with the pilot interval being 7 and 6, respectively, is also provided. It is seen that Algorithm 1 with $J = 1$ using joint pilot design achieves almost the same performance as LS with $K = 87$. Therefore, the joint design can reduce the pilot overhead by 71 pilots and improve the spectrum efficiency by 13.9%, thus leading to additional 2.4% improvement compared with the pilot design assuming equal pilot power in [14].

VI. Conclusion

In this correspondence, we have investigated the joint design of pilot power and pilot pattern based on the rule of MIP. The pilot design has been formulated as a joint optimization problem, which is then decoupled into tractable sequential formations. Given a pilot pattern, we have formulated the design of pilot power as an SOCP problem. Then, we have proposed a joint design algorithm. Simulation results have verified the effectiveness of the proposed algorithm and shown that the proposed algorithm can achieve better channel estimation performance and further improve the spectrum efficiency by 2.4%, compared with existing algorithms assuming equal pilot power.

References

[1] X. Kang, Y.-C. Liang, A. Nallanathan, H. K. Garg, and R. Zhang, "Optimal power allocation for fading channels in cognitive radio networks: Ergodic capacity and outage capacity," *IEEE Trans. Wireless Commun.*, vol. 8, no. 2, pp. 940–950, Feb. 2009.

[2] Y. Liang, K. C. Chen, G. Y. Li, and P. Mahonen, "Cognitive radio networking and communications: An overview," *IEEE Trans. Veh. Technol.*, vol. 60, no. 7, pp. 3386–3407, Sep. 2011.

[3] D. Hu, L. He, and X. Wang, "An efficient pilot design method for OFDM-based cognitive radio systems," *IEEE Trans. Wireless Commun.*, vol. 10, no. 4, pp. 1252–1259, Apr. 2011.

[4] E. Manasseh, S. Ohno, and M. Nakamoto, "Pilot symbol assisted channel estimation for OFDM-based cognitive radio systems," *EURASIP J. Adv. Signal Process.*, vol. 51, no. 1, pp. 51:1–51:11, Mar. 2013.

[5] J. C. Chen and C. K. Wen, "A novel cognitive radio adaptation for wireless multicarrier systems," *IEEE Commun. Lett.*, vol. 14, no. 7, pp. 629–631, Jul. 2010.

[6] C. R. Berger, Z. Wang, J. Huang, and S. Zhou, "Application of compressive sensing to sparse channel estimation," *IEEE Commun. Mag.*, vol. 48, no. 11, pp. 164–174, Nov. 2010.

[7] C. Qi and L. Wu, "Uplink channel estimation for massive MIMO systems exploring joint channel sparsity," *Electron. Lett.*, vol. 50, no. 23, pp. 1770–1772, Nov. 2014.

[8] P. Pakrooh, A. Amini, and F. Marvasti, "OFDM pilot allocation for sparse channel estimation," *EURASIP J. Adv. Signal Process.*, vol. 59, no. 1, pp. 59:1–59:9, Mar. 2012.

[9] C. Qi and L. Wu, "A study of deterministic pilot allocation for sparse channel estimation in OFDM systems," *IEEE Commun. Lett.*, vol. 16, no. 5, pp. 742–744, May 2012.

[10] J.-C. Chen, C.-K. Wen, and P. Ting, "An efficient pilot design scheme for sparse channel estimation in OFDM systems," *IEEE Commun. Lett.*, vol. 17, no. 7, pp. 1352–1355, Jul. 2013.

[11] C. Qi and L. Wu, "Optimized pilot placement for sparse channel estimation in OFDM systems," *IEEE Signal Process. Lett.*, vol. 18, no. 12, pp. 749–752, Dec. 2011.

[12] X. He, R. Song, and W.-P. Zhu, "Pilot allocation for sparse channel estimation in MIMO-OFDM systems," *IEEE Trans. Circuits Syst. II, Exp. Briefs*, vol. 60, no. 9, pp. 612–616, Sep. 2013.

[13] P. Cheng *et al.*, "Sparse channel estimation for OFDM transmission over two-way relay networks," in *Proc. IEEE ICC*, Ottawa, ON, Canada, Jun. 2012, pp. 3948–3953.

[14] C. Qi, G. Yue, L. Wu, and A. Nallanathan, "Pilot design for sparse channel estimation in OFDM-based cognitive radio systems," *IEEE Trans. Veh. Technol.*, vol. 63, no. 2, pp. 982–987, Feb. 2014.

[15] W. U. Bajwa, J. Haupt, A. M. Sayeed, and R. Nowak, "Compressed channel sensing: A new approach to estimating sparse multipath channels," *Proc. IEEE*, vol. 98, no. 6, pp. 1058–1076, Jun. 2010.

[16] D. Hu, X. Wang, and L. He, "A new sparse channel estimation and tracking method for time-varying OFDM systems," *IEEE Trans. Veh. Technol.*, vol. 62, no. 9, pp. 4648–4653, Nov. 2013.

[17] E. J. Candes and T. Tao, "Decoding by linear programming," *IEEE Trans. Inf. Theory*, vol. 51, no. 12, pp. 4203–4215, Dec. 2005.

[18] T. Cai and L. Wang, "Orthogonal matching pursuit for sparse signal recovery with noise," *IEEE Trans. Inf. Theory*, vol. 57, no. 7, pp. 4680–4688, Jul. 2011.

[19] M.-S. Lobo, L. Vandenberghe, S. Boyd, and H. Lebret, "Applications of second-order cone programming," *Linear Algebra Appl.*, vol. 284, no. 1–3, pp. 193–228, Nov. 1998.

AUTHOR QUERY

NO QUERY.

Correspondence

Joint Design of Pilot Power and Pilot Pattern for Sparse Cognitive Radio Systems

Chenhao Qi, *Member, IEEE*, Lenan Wu, Yongming Huang, *Member, IEEE*, and A. Nallanathan, *Senior Member, IEEE*

***Abstract*—Existing works design the pilot pattern for sparse channel estimation, assuming that the power of all pilots is equal. However, equal power allocation is not optimal in cognitive radio (CR) systems. In this correspondence, we jointly design the pilot power and pilot pattern for sparse channel estimation in orthogonal-frequency-division-multiplexing-based CR systems, based on the rule of mutual incoherence property that minimizes the coherence of the measurement matrix used for the sparse recovery. Under the sum power constraint and peak power constraint, the pilot design is formulated as a joint optimization problem, which is then decoupled into tractable sequential formations. Given a pilot pattern, we formulate the design of pilot power as a second-order cone programming. Then, we propose a joint design algorithm, which includes discrete optimization for pilot pattern and continuous optimization for pilot power. Simulation results show that the proposed algorithm can achieve better channel estimation performance in terms of mean square error and bit error rate and can further improve the spectrum efficiency by 2.4%, compared with existing algorithms assuming equal pilot power.**

***Index Terms*—Cognitive radio (CR), compressed sensing (CS), orthogonal frequency-division multiplexing (OFDM), pilot design, sparse channel estimation.**

I. Introduction

Radio spectrum is a precious and limited resource for wireless communications. In attempts to relieve the spectrum shortage, the concept of cognitive radio (CR) is proposed, which allows secondary users (SUs) to opportunistically access the spectrum that is originally allocated to primary users (PUs). SUs start communications with each other when the spectrum is not used by any PU. Therefore, CR can improve the usage of existing frquency bands without allocating a new spectrum resource [1]. On the other hand, with the great capability in combating frequency-selective fading and the high flexibility in allocating transmit resources, orthogonal frequency-division multiplexing (OFDM) has been suggested as a competitive candidate in CR systems [2]. In OFDM-based CR systems, the subcarriers are noncontiguous. Hence, the efficient design of pilots including pilot pattern and pilot power is crucial to the performance of channel estimation and data detection. In [3], a scheme to design pilot symbols for OFDM-based CR systems is proposed, where the pilot design assuming equal pilot power is formulated as an optimization problem that minimizes the upper bound related to the mean square error (MSE) of least squares (LS) channel estimation. In [4], a scheme that utilizes cross entropy (CE) optimization together with the analytical pilot power optimization is proposed to design pilot symbols to reduce the MSE of the LS channel estimation. In [5], parameter adaptation for wireless multicarrier-based CR systems is investigated where the CE method is demonstrated to outperform the genetic algorithm (GA) and particle swarm optimization (PSO). However, all these literatures are based on the LS channel estimation.

Recently, sparse channel estimation that exploits the inherent sparse property of wireless multipath channels and applies the compressed sensing (CS) techniques for channel estimation has been proven to improve the channel estimation performance and reduce the pilot overhead compared with the LS method [6], [7]. To further improve the performance of sparse channel estimation, one effective approach is to optimize the pilot design. In [8] and [9], it has been shown that the pilot pattern generated from the cyclic different set (CDS) is optimal and have proposed a scheme to obtain a near-optimal pilot pattern when the CDS does not exist. In [10] and [11], two pilot design schemes based on CE optimization and stochastic approximation, respectively, are proposed to minimize the MSE of sparse channel estimation using the channel data. In [12], a pilot allocation method based on the GA and a shifting mechanism is proposed for sparse channel estimation in multiple-input–multiple-output OFDM systems. In [13], a pilot design scheme for OFDM transmission over two-way relay networks is presented. In [14], sparse channel estimation is first introduced in OFDM-based CR systems. Based on the results of spectrum sensing, a scheme using constrained CE optimization is proposed to obtain an optimized pilot pattern. In particular, it is shown in [14] that sparse channel estimation can achieve 11.5% improvement in spectrum efficiency with the same channel estimation performance compared with the LS channel estimation. However, all existing works design the pilot pattern for sparse channel estimation assuming that the power of pilots is equal.

In this correspondence, based on the work of Qi et al. in [14], we further consider the pilot power optimization for sparse channel estimation in OFDM-based CR systems. Note that the CR system employing sparse channel estimation is termed as the sparse CR system in this work. We jointly design the pilot power and pilot pattern based on the rule of mutual incoherence property (MIP) that minimizes the coherence of the measurement matrix used for the sparse recovery. Under the sum power constraint and peak power constraint, the pilot design is formulated as a joint optimization problem, which is then decoupled into tractable sequential formations. Given a pilot pattern, we formulate the design of pilot power as a second-order cone programming (SOCP). Then, we propose a joint design algorithm, which includes discrete optimization for pilot pattern and continuous optimization for pilot power.

The notations used in this correspondence are defined as follows. Symbols for matrices (uppercase) and vectors (lowercase) are in boldface. $(\cdot)^T$, $(\cdot)^H$, $\mathrm{diag}\{\cdot\}$, $\boldsymbol{I}_L$, $\setminus$, $\mathbb{C}^{M\times N}$, $\mathbf{0}^{M\times N}$, $\mathcal{CN}$, $|\cdot|$, $\|\cdot\|_0$, $\|\cdot\|_2$, $\|\cdot\|_\infty$, $\mathrm{Re}\{\cdot\}$, and $\mathrm{Im}\{\cdot\}$ denote the matrix transpose, conjugate transpose (Hermitian), the diagonal matrix, the identity matrix of size L, the set exclusion, the set of $M \times N$ complex matrices, the $M \times N$ zero matrix, the complex Gaussian distribution, the absolute

Manuscript received February 27, 2014; revised July 4, 2014, and September 24, 2014; accepted November 16, 2014.This work was supported in part by the National Natural Science Foundation of China under Grants 61302097 and 61422105, by the Ph.D. Programs Foundation of the Ministry of Education of China under Grant 20120092120014, and by the Natural Science Foundation of Jiangsu Province under Grant BK20130019. The review of this paper was coordinated by Prof. X. Wang.

C. Qi, L. Wu, and Y. Huang are with the School of Information Science and Engineering, Southeast University, Nanjing 210096, China (e-mail: qch@seu.edu.cn; wuln@seu.edu.cn; huangym@seu.edu.cn).

A. Nallanathan is with the Department of Informatics, King's College London, London WC2R 2LS, U.K. (e-mail: nallanathan@ieee.org).

Color versions of one or more of the figures in this paper are available online at http://ieeexplore.ieee.org.

Digital Object Identifier 10.1109/TVT.2014.2374692

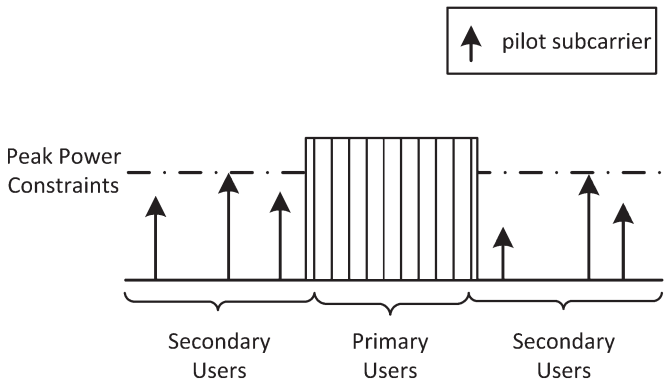

Fig. 1. Joint design of pilot power and pilot pattern for SUs under peak power constraint.

value, the ℓ_0 norm, the ℓ_2 norm, the ℓ_∞ norm, real part, and imaginary part, respectively. $\mathcal{O}(\cdot)$ denotes the order of complexity. $\hat{\phi}$ denotes the estimate of the parameter of interest ϕ.

II. Problem Formulation

We consider an OFDM-based CR system employing sparse channel estimation to exploit the inherent sparse property of wireless multipath channels. The channel is modeled as an finite impulse response filter with the channel impulse response (CIR) to be

$$\boldsymbol{h} = [h(1), h(2), \ldots, h(L)]^T. \tag{1}$$

$\boldsymbol{h}$ is sparse if the number of nonzero entries of $\boldsymbol{h}$, which is denoted as S, is much smaller than the channel length L ($S \ll L$).

Similar to [3] and [14], we assume ideal spectrum sensing without false alarm or missing detection. Based on the results of spectrum sensing, the OFDM subcarriers occupied by PUs are first deactivated. From the active subcarriers, we use some subcarriers to transmit pilot symbols and the others to transmit data symbols for SUs. We assume that the secondary transmitters of SUs broadcast the results of pilot design to the secondary receivers of SUs through control signaling.

Suppose an OFDM-based CR system with N subcarriers. After deactivating subcarriers occupied by PUs, there are $M(M \leq N)$ active subcarriers available for SUs. We denote these active subcarriers as $\mathcal{C}\{c_1, c_2, \ldots, c_M\}$, where $\mathcal{C} \subseteq \mathcal{N}$ with $\mathcal{N} = \{1, 2, \ldots, N\}$. Without loss of generality, we suppose $1 \leq c_1 < c_2 < \cdots < c_M \leq N$. From $\mathcal{C}$, we select $K(K \leq M)$ pilot subcarriers indexed by $c_{p_1}, c_{p_2}, \ldots, c_{p_K}$ $(1 \leq p_1 < p_2 < \cdots < p_K \leq M)$ to transmit pilot symbols for frequency-domain pilot-assisted channel estimation, as shown in Fig. 1. The indexes of pilot subcarriers make up a pilot pattern $\boldsymbol{p} = \{c_{p_1}, c_{p_2}, \ldots, c_{p_K}\}$, where $\boldsymbol{p} \subseteq \mathcal{C}$. We define the set of all possible pilot patterns as $\mathcal{P} \triangleq \{\boldsymbol{w} | \boldsymbol{w} \subseteq \mathcal{C},\ \|\boldsymbol{w}\|_0 = K\}$. Then, we have $\boldsymbol{p} \subset \mathcal{P}$. Note that all existing literatures of pilot design for sparse channel estimation are all based on the equal pilot power assumption. However, in OFDM-based CR systems, the pilot power can be different, as shown in Fig. 1, where the equal pilot power is not necessarily optimal. In this paper, we will study the joint design of pilot power and pilot pattern.

We denote the transmit pilot symbols and the receive pilot symbols as $\boldsymbol{x} = [x(c_{p_1}), x(c_{p_2}), \ldots, x(c_{p_K})]^T$ and $\boldsymbol{y} = [y(c_{p_1}), y(c_{p_2}), \ldots, y(c_{p_K})]^T$, respectively. For LS channel estimation, we first acquire channel frequency response (CFR) at pilot subcarriers by $\{y(i)/x(i),\ i \in \boldsymbol{p}\}$ and then make interpolations for the rest of the subcarriers. However, it usually demands a large number of pilots, i.e., $K > L$, so that the interpolations can approximate the true value of CFR. The relation between the transmit pilots and the receive pilots can be written in matrix notation as

$$\boldsymbol{y} = \boldsymbol{X}\boldsymbol{F}\boldsymbol{h} + \boldsymbol{\eta} \tag{2}$$

where

$$\boldsymbol{X} = \mathrm{diag}\left\{x\left(c_{p_1}\right), x\left(c_{p_2}\right), \ldots, x\left(c_{p_K}\right)\right\} \tag{3}$$

$$\boldsymbol{\eta} = [\eta(1), \eta(2), \ldots, \eta(K)]^T \sim \mathcal{CN}(\boldsymbol{0}, \sigma^2 \boldsymbol{I}_K) \tag{4}$$

and $\boldsymbol{F}$ is a discrete Fourier transform submatrix given by

$$\boldsymbol{F} = \frac{1}{\sqrt{N}} \begin{bmatrix} 1 & \omega^{c_{p_1}} & \cdots & \omega^{c_{p_1}(L-1)} \\ 1 & \omega^{c_{p_2}} & \cdots & \omega^{c_{p_2}(L-1)} \\ \vdots & \vdots & \ddots & \vdots \\ 1 & \omega^{c_{p_K}} & \cdots & \omega^{c_{p_K}(L-1)} \end{bmatrix}$$

where $\omega = e^{-j2\pi/N}$. We further denote

$$\boldsymbol{A} \triangleq \boldsymbol{X}\boldsymbol{F}. \tag{5}$$

Then, (2) can be written as

$$\boldsymbol{y} = \boldsymbol{A}\boldsymbol{h} + \boldsymbol{\eta}. \tag{6}$$

If $L \leq K \leq M$ and $\boldsymbol{A}$ has full column rank, (6) can be solved by LS, which essentially employs the fast Fourier transform interpolations with the estimated CIR given by

$$\hat{\boldsymbol{h}}_{\mathrm{LS}} = (\boldsymbol{A}^H \boldsymbol{A})^{-1} \boldsymbol{A}^H \boldsymbol{y}. \tag{7}$$

However, a large number of pilots is required. The CS theory shows that we can reduce the number of pilots, i.e., $2S < K < L$, by exploring the sparse property of wireless channels. To identify the positions of the S nonzero entries as well as estimating the coefficients of the S nonzero entries, which results in totally $2S$ unknown parameters, we have to use at least $K > 2S$ pilots. With this condition, we can apply CS algorithms, e.g., orthogonal matching pursuit (OMP), to estimate $\boldsymbol{h}$. Existing works have already shown that the CS algorithms outperform LS for channel estimation [15], [16].

The restrict isometry property (RIP) shows that $\boldsymbol{h}$ in (6) can be recovered from the noiseless measurement $\boldsymbol{y}(\boldsymbol{\eta} = 0)$ with a high probability if the measurement matrix $\boldsymbol{A}$ satisfies the RIP [17]. It is said that $\boldsymbol{A} \in \mathbb{C}^{K \times L}$ in (6) satisfies the RIP if there exists a constant $\delta(0 < \delta < 1)$ such that

$$(1 - \delta)\|\boldsymbol{u}\|_2^2 \leq \|\boldsymbol{A}\boldsymbol{u}\|_2^2 \leq (1 + \delta)\|\boldsymbol{u}\|_2^2 \tag{8}$$

holds for all S-sparse[1] vectors $\boldsymbol{u} \in \mathbb{C}^L$. However, it is computationally infeasible to check whether a given matrix $\boldsymbol{A}$ satisfies the RIP. Alternatively, according to [18], we can minimize the coherence of $\boldsymbol{A}$, which is known as the MIP. The MIP condition is stronger than the RIP in that the MIP implies the RIP but the converse is not true [18]. Moreover, the MIP is more intuitive and practical than the RIP. Here, we consider the pilot design including joint pilot power allocation and pilot pattern optimization with respect to the MIP.

Given a pilot pattern, i.e.,

$$\boldsymbol{p} = \{c_{p_1}, c_{p_2}, \ldots, c_{p_K}\} \tag{9}$$

and a pilot power vector, i.e.,

$$\boldsymbol{v} = \{v_1, v_2, \ldots, v_K\} \tag{10}$$

[1] $\boldsymbol{u} \in \mathbb{C}^L$ is said to be S-sparse ($S \ll L$) if the number of nonzero entries of $\boldsymbol{u}$ is equal to S or smaller than S.

with v_i denoting the power of the ith pilot symbol transmitted by the c_{p_i}th subcarrier, i.e.,

$$v_i \triangleq |x(c_{p_i})|^2, \quad i = 1, 2, \ldots, K \tag{11}$$

we define the coherence of $\boldsymbol{A}$ as the maximum absolute correlation between any two different columns of $\boldsymbol{A}$, i.e.,

$$\begin{aligned} g(\boldsymbol{p}, \boldsymbol{v}) &\triangleq \max_{0 \le m < n \le L-1} |\langle A(m), A(n) \rangle| \\ &= \max_{0 \le m < n \le L-1} \left| \sum_{i=1}^{K} v_i \omega^{c_{p_i}(n-m)} \right| \Big/ \sum_{i=1}^{K} v_i \end{aligned} \tag{12}$$

where $\langle A(m), A(n) \rangle$ denotes the normalized inner product between the mth column $A(m)$ and the nth column $A(n)$ of $\boldsymbol{A}$, i.e.,

$$\langle A(m), A(n) \rangle \triangleq \frac{A^H(m) A(n)}{\|A(m)\|_2 \|A(n)\|_2}. \tag{13}$$

Let $d = n - m$ and $\Lambda = \{1, 2, \ldots, L-1\}$. Then, (12) can be rewritten as

$$g(\boldsymbol{p}, \boldsymbol{v}) = \max_{d \in \Lambda} \left| \sum_{i=1}^{K} v_i \omega^{c_{p_i} d} \right| \Big/ \sum_{i=1}^{K} v_i. \tag{14}$$

According to the MIP, the objective for the pilot design is to minimize the coherence of $\boldsymbol{A}$, i.e., $\min_{\boldsymbol{p}, \boldsymbol{v}} \ g(\boldsymbol{p}, \boldsymbol{v})$. The constraint for the integer vector $\boldsymbol{p}$ is $\boldsymbol{p} \subset \mathcal{P}$. Suppose the sum power of all pilot symbols is

$$\sum_{i=1}^{K} v_i = V_T \tag{15}$$

where V_T is the prespecified sum power constraint of SUs. Obviously, (15) is more general in practical OFDM-based CR systems than simply assuming

$$v_1 = v_2 = \cdots = v_K = \frac{V_T}{K} \tag{16}$$

in current literatures [8]–[10]. On the other hand, SUs should properly control the peak power of pilot subcarriers regarding the linear region of power amplifiers. The power of pilot subcarriers cannot be too large or too small. As shown in Fig. 1, we denote V_H as the peak power constraint related to the saturation power of the power amplifier. Moreover, the pilot power should be greater than a threshold V_L, which is related to the cutoff power of the power amplifier as well as the noise and interference level around SUs. In particular, $V_L = 0$ can be regarded as a special case. Hence, we have

$$V_L \le v_i \le V_H, \quad i = 1, 2, \ldots, K. \tag{17}$$

With these constraints, the pilot design in OFDM-based CR systems can be formulated as

$$\begin{aligned} \min_{\boldsymbol{p}, \boldsymbol{v}} \quad & g(\boldsymbol{p}, \boldsymbol{v}) \\ \text{s.t.} \quad & \boldsymbol{p} \subset \mathcal{P} \\ & \sum_{i=1}^{K} v_i = V_T, \ V_L \le v_i \le V_H \end{aligned} \tag{18}$$

which involves the joint optimization of the discrete integer vector $\boldsymbol{p}$ and the continuous real-valued positive vector $\boldsymbol{v}$. Note that unlike most literatures, investigating the optimal power allocation to maximize the achievable rate of CR systems, in this paper, we focus on the pilot design for sparse channel estimation, where the design of data subcarriers is out of the scope of this work.

Apparently, it is analytically intractable to get a solution from (18). We now decouple this joint optimization problem with the following two kinds of sequential formulations.

1) Given a $\tilde{\boldsymbol{p}} \subset \mathcal{P}$, we first get

$$\begin{aligned} & g_v(\tilde{\boldsymbol{p}}) \triangleq \min_{\boldsymbol{v}} g(\tilde{\boldsymbol{p}}, \boldsymbol{v}) \\ & \text{s.t.} \quad \sum_{i=1}^{K} v_i = V_T, \ V_L \le v_i \le V_H \end{aligned} \tag{19}$$

then we solve

$$\min_{\tilde{\boldsymbol{p}} \subset \mathcal{P}} g_v(\tilde{\boldsymbol{p}}) \tag{20}$$

to get an optimal $\boldsymbol{p}$. Meanwhile, the corresponding $\boldsymbol{v}$ is also obtained.

2) Given a feasible $\tilde{\boldsymbol{v}}$, we first get

$$g_p(\tilde{\boldsymbol{v}}) \triangleq \min_{\boldsymbol{p} \subset \mathcal{P}} g(\boldsymbol{p}, \tilde{\boldsymbol{v}}) \tag{21}$$

then we solve

$$\begin{aligned} \min_{\tilde{\boldsymbol{v}}} \quad & g_p(\tilde{\boldsymbol{v}}) \\ \text{s.t.} \quad & \sum_{i=1}^{K} \tilde{v}_i = V_T, \ V_L \le \tilde{v}_i \le V_H \end{aligned} \tag{22}$$

to get an optimal $\boldsymbol{v}$. Meanwhile, the corresponding $\boldsymbol{p}$ is also obtained.

Comparing $\boldsymbol{p} \subset \mathcal{P}$ with the constraints in (15) and (17), it can be seen that $\boldsymbol{p}$ is less difficult to enumerate than $\boldsymbol{v}$. Therefore, it is better to decouple the joint optimization problem described by (18) with the first kind of formulations described by (19) and (20).

III. Pilot Power Allocation

Regarding (19), with a given pilot pattern $\tilde{\boldsymbol{p}} \subset \mathcal{P}$, we first generate a table, i.e.,

$$\boldsymbol{G} = \begin{bmatrix} \omega^{c_1} & \omega^{c_2} & \cdots & \omega^{c_M} \\ \omega^{2c_1} & \omega^{2c_2} & \cdots & \omega^{2c_M} \\ \vdots & \vdots & \ddots & \vdots \\ \omega^{(L-1)c_1} & \omega^{(L-1)c_2} & \cdots & \omega^{(L-1)c_M} \end{bmatrix} \tag{23}$$

where $\omega = e^{-j2\pi/N}$. Once N, L and $\mathcal{C}$ are given, $\boldsymbol{G}$ is determined.

We look up $\boldsymbol{G}$ and select the corresponding K columns indexed by $\tilde{\boldsymbol{p}}$ from $\boldsymbol{G}$, making up a $L-1$ by K submatrix $\boldsymbol{G}(\tilde{\boldsymbol{p}})$. Then, from (14), we have

$$g(\tilde{\boldsymbol{p}}, \boldsymbol{v}) = \frac{1}{V_T} \|\boldsymbol{G}(\tilde{\boldsymbol{p}}) \boldsymbol{v}\|_\infty. \tag{24}$$

Therefore, (19) is equivalent to

$$\begin{aligned} \min_{\boldsymbol{v}} \quad & \|\boldsymbol{G}(\tilde{\boldsymbol{p}}) \boldsymbol{v}\|_\infty \\ \text{s.t.} \quad & \sum_{i=1}^{K} v_i = V_T, \ V_L \le v_i \le V_H \end{aligned} \tag{25}$$

where $\tilde{\boldsymbol{p}}$ is given, and $\boldsymbol{G}(\tilde{\boldsymbol{p}})$ is a complex-valued submatrix fast generated by looking up $\boldsymbol{G}$. Let $\boldsymbol{b}_i$ denote the ith row of $\boldsymbol{G}(\tilde{\boldsymbol{p}})$, $i = 1, 2, \ldots, L-1$. We further denote

$$\boldsymbol{B}_i = \begin{bmatrix} \mathrm{Re}\{\boldsymbol{b}_i\} \\ \mathrm{Im}\{\boldsymbol{b}_i\} \end{bmatrix},\ i = 1, 2, \ldots, L-1 \tag{26}$$

which is a real-valued matrix with two rows and K columns. Then, (25) can be converted into a real-valued optimization problem as

$$\begin{aligned} \min_{z}\ & z \\ \text{s.t.}\quad & \|\boldsymbol{B}_i \boldsymbol{v}\|_2 \le z,\ i = 1, 2, \ldots, L-1 \\ & \sum_{i=1}^{K} v_i = V_T,\ V_L \le v_i \le V_H \end{aligned} \tag{27}$$

which is an SOCP optimization problem that contains $L-1$ second-order conic constraints and some linear constraints. Typically, it can be solved by SOCP solvers, e.g., MOSEK. Then, we can obtain feasible solutions as $\tilde{z}$ and $\tilde{\boldsymbol{v}}$ from (27), where $g_v(\tilde{\boldsymbol{p}}) = \tilde{z}$.

IV. Joint Pilot Design

If M and K are not small enough, $\mathcal{P}$ can be a huge set. For example, if $M = 512$ and $K = 16$, $\|\mathcal{P}\|_0 = \binom{512}{16} = 8.4 \times 10^{29}$. It is impossible for SUs to store $\mathcal{P}$ into the memory and check them one by one until the best $\boldsymbol{p} \subset \mathcal{P}$ is found. Furthermore, it is very computationally inefficient to implement the exhaustive search from such huge space, particularly for SUs equipped with power-constrained mobile devices.

The proposed joint design algorithm including discrete optimization for pilot pattern and continuous optimization for pilot power is described in Algorithm 1. At first, we input system parameters $\mathcal{C}$, N, M, K, L, J, T_1, and T_2, where T_1 and T_2 represent the number of outer-loop and inner-loop iterations, respectively. Each outer-loop iteration includes T_2 inner-loop iterations. Then, we initialize a zero-matrix $\boldsymbol{D}$ to store the results of optimized pilot patterns after running inner-loop iterations. Each row of $\boldsymbol{D}$ stores a pilot pattern $\boldsymbol{p}$, with the corresponding objective value $g_v(\boldsymbol{p})$ stored in $\boldsymbol{r}$, which is initialized to be a zero vector. Then, we generate a table $\boldsymbol{G}$ according to (23). At each outer-loop iteration, indicated from step 4 to step 16, we start by randomly generating a pilot pattern $\boldsymbol{p} \subset \mathcal{P}$. By introducing the randomness to the algorithm so that it starts from different initial pilot patterns, we can avoid that the algorithm falls into local optimums. As T_1 increases to infinity, the algorithm will converge to the global optimum. Then, we use the inner-loop iterations from step 6 to step 14 to obtain an optimized pilot pattern $\boldsymbol{p}$, which is stored in each row of $\boldsymbol{D}$ with the corresponding objective value $g_v(\boldsymbol{p})$ stored in $\boldsymbol{r}$, indicated by step 15. After we finish the outer-loop iterations, we select the minimum from $\boldsymbol{r}$ and output the corresponding row of $\boldsymbol{D}$ as the designed pilot pattern $\boldsymbol{p}_o$, indicated by step 17 and step 18. We then substitute $\boldsymbol{p}_o$ into (27) to design the pilot power.

Algorithm 1 Joint Design of Pilot Power and Pilot Pattern

1: Input: $\mathcal{C}$, N, M, K, L, J, T_1, T_2.
2: Initializations: $\boldsymbol{D} \Leftarrow \boldsymbol{0}^{T_1 \times K}$. $\boldsymbol{r} \Leftarrow \boldsymbol{0}^{T_1}$.
3: Generate $\boldsymbol{G}$ according to (23).
4: **for** $l = 1, 2, \ldots, T_1$
5: randomly generate $\boldsymbol{p} \subset \mathcal{P}$. $\boldsymbol{p}^* \Leftarrow \boldsymbol{0}^K$.
6: **for** $n = 1, 2, \ldots, T_2$
7: **if** $\boldsymbol{p} = \boldsymbol{p}^*$
8: break.
9: **end if**
10: $\boldsymbol{p}^* \Leftarrow \boldsymbol{p}$.
11: **for** $k = 1, 2, \ldots, K/J$
12: Obtain $\hat{\boldsymbol{p}}_{\boldsymbol{p},k}$ according to (31). $\boldsymbol{p} \Leftarrow \hat{\boldsymbol{p}}_{\boldsymbol{p},k}$.
13: **end for**(k)
14: **end for**(n)
15: $D(l) \Leftarrow \boldsymbol{p}$. $r(l) \Leftarrow g_v(\boldsymbol{p})$.
16: **end for**(l)
17: $t = \arg\min_{i=1,2,\ldots,T_1} r(i)$.
18: Output $\boldsymbol{p}_o = D(t)$ as the designed pilot pattern.
19: Substitute $\boldsymbol{p}_o$ into (27) to design the pilot power.

Here, we use an auxiliary vector $\boldsymbol{p}^*$, which always records the pilot pattern obtained from the previous inner-loop iteration. If we find that $\boldsymbol{p}$ is exactly the same as $\boldsymbol{p}^*$, which means we did not get a new pilot pattern, there is no need to continue the inner-loop iterations because the results thereafter will be exactly the same. Then, we break from the inner-loop iterations. These procedures are indicated from step 7 to step 10. Additionally, we have to reset $\boldsymbol{p}^*$ by $\boldsymbol{p}^* \Leftarrow \boldsymbol{0}^K$ at the start of each outer-loop iteration. This way, we can save the CPU running time and therefore improve the efficiency by skipping the same routine.

The main contribution of Algorithm 1 is the group update of entries of $\boldsymbol{p}$, which is shown from step 11 to step 13. The update of $\boldsymbol{p}$ is implemented in a group of J entries each time, where K is divisible by J, i.e., K/J is a positive integer. For $k = 1, 2, \ldots, K/J$, given the latest $\boldsymbol{p}$ from the last inner-loop iteration, we update the kth group of entries of $\boldsymbol{p}$ with the best group selected from

$$\mathcal{W} = \{\boldsymbol{w} | \boldsymbol{w} \subseteq \Psi,\ \|\boldsymbol{w}\|_0 = J\} \tag{28}$$

where

$$\Psi = \mathcal{C} \setminus \{p(i) | i = 1, 2, \ldots, K, i \notin \Phi\} \tag{29}$$

$$\Phi = \{kJ - J + 1, kJ - J + 2, \ldots, kJ\}. \tag{30}$$

Mathematically, the resultant pilot pattern $\hat{\boldsymbol{p}}_{\boldsymbol{p},k}$ with the update of the kth group of entries is given by

$$\hat{\boldsymbol{p}}_{\boldsymbol{p},k} = \arg \min_{\substack{\tilde{\boldsymbol{p}} \\ \tilde{p}(i) = p(i),\ i = 1,2,\ldots,K, i \notin \Phi \\ \{\tilde{p}(i), i \in \Phi\} \subset \mathcal{W}}} g_v(\tilde{\boldsymbol{p}}) \tag{31}$$

where the computation of $g_v(\tilde{\boldsymbol{p}})$ is provided in Section III. After we obtain $\hat{\boldsymbol{p}}_{\boldsymbol{p},k}$ for given $\boldsymbol{p}$ and k, we update $\boldsymbol{p}$ by $\boldsymbol{p} \Leftarrow \hat{\boldsymbol{p}}_{\boldsymbol{p},k}$.

The complexity for pilot power allocation given a pilot pattern in (27) is $\mathcal{O}((L-1)^{1.5}(K+1)^3)$. Therefore, the computational complexity for Algorithm 1 is

$$\mathcal{O}\left(T_1 T_2 (L-1)^{1.5} (K+1)^3 \frac{K}{J} \binom{M-K+J}{J}\right) \tag{32}$$

suppose that T_2 is small enough [19]. If T_2 is large, the inner-loop iterations will terminate itself by procedures from step 7 to step 9, leading to even lower complexity than (32).

Remark: If we set $J = K$, Algorithm 1 degenerates to be the exhaustive search, where $\|\mathcal{W}\|_0 = \binom{M}{K}$, and $\|\Phi\|_0 = K$. In this case, no matter what T_1 and T_2 are, they are equivalent to $T_1 = T_2 = 1$, resulting in $\mathcal{O}(\binom{M-K+J}{J})$, which is the extraordinarily high complexity of the exhaustive search. In practice, we usually set $J = 1$ or $J = 2$ to reduce the complexity. For example, if $J = 1$, (32) reduces to a polynomial complexity, i.e., $\mathcal{O}(T_1 T_2 (L-1)^{1.5}(K+1)^3 K(M-K+1))$.

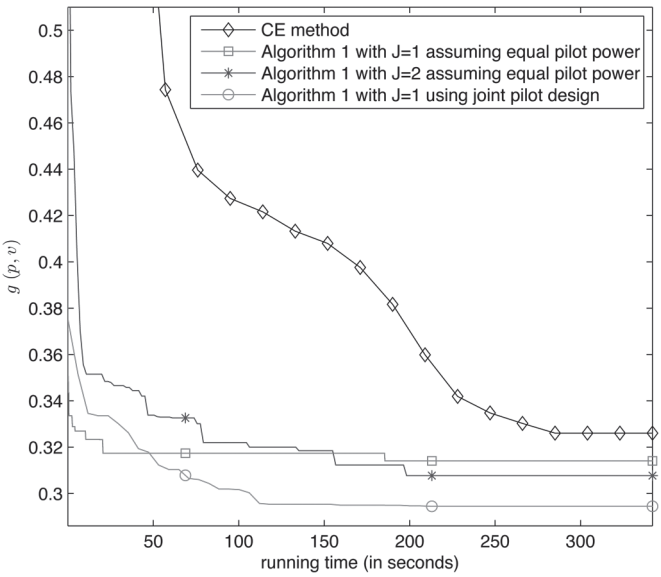

Fig. 2. Comparisons of convergence and complexity for different algorithms or parameters.

V. Simulation Results

To compare this work with [14], we set the same system parameters as [14]. We consider an OFDM-based CR system with $N = 1024$ subcarriers. After ideal spectrum sensing, there are $M = 512$ active subcarriers available for SUs, including three subcarrier blocks, i.e., $\mathcal{B}_1 = \{1, 2, 3, \ldots, 256\}$, $\mathcal{B}_2 = \{513, 514, \ldots, 640\}$, $\mathcal{B}_3 = \{897, 898, \ldots, 1024\}$, with the number of contiguous subcarriers of each block being 256, 128, and 128, respectively. From $\mathcal{C} = \mathcal{B}_1 \cup \mathcal{B}_2 \cup \mathcal{B}_3$, which can also be regarded as the union of several active CR subbands for SUs, we want to select $K = 16$ pilot subcarriers for frequency-domain pilot-assisted channel estimation. A sparse multipath channel $\boldsymbol{h}$ is generated with $L = 60$ taps, where $S = 5$ dominant nonzero channel taps are randomly placed among L taps. The channel gain of each path is independent and identically distributed complex Gaussian distributed with unit variance, i.e., $\mathcal{CN}(0, 1)$. Quaternary phase-shift keying modulation is employed in the simulations.

To evaluate the performance of Algorithm 1, we first compare it with the CE method [14] assuming equal pilot power indicated by (16), where the joint pilot design is simplified to be the pilot pattern design. We set $V_T = 1$, which means that the sum power of pilot subcarriers is normalized. We set $V_L = 0.03$ and $V_H = 0.1$ so that the pilot power does not vary too much. The steps for optimal pilot power allocation in Algorithm 1 are skipped by directly substituting $v_1 = v_2 = \cdots = v_{16} = 0.0625$ into (24). The parameters of the CE method are selected to be the best in [14], where the maximum number of iterations, the number of random samples, the sample quantile, and the smoothing factor are set to be 50, 100 000, 0.001, and 0.3, respectively. It can be seen in Fig. 2 that Algorithm 1 is much faster convergent than the CE method. Here, we compare the convergence speed with respect to the running time instead of the number of iterations, because the running time of each iteration is different for different algorithms or parameters. Since we run the simulations under the exact same computer hardware and software, the running time is proportional to the computational complexity. We set $T_1 = 1000$ and $T_2 = 15$ for Algorithm 1. Once the running time, i.e., 342 s, which is the running time for the CE method [14], is reached, we terminate Algorithm 1 so that we can compare Algorithm 1 with the CE method under the same computational complexity. As shown in Fig. 2, Algorithm 1 with $J = 1$ can achieve the best performance of the CE method in no more than 10 s, which indicates that Algorithm 1 is 34 times faster than the CE method and, therefore, is much more efficient and powerful. Since it has already been demonstrated in [5] that the CE method outperforms GA and PSO, Algorithm 1 is a remarkable candidate for integer optimization with its applications not restricted to the pilot design. As shown in Fig. 2, although Algorithm 1 with $J = 2$ converges slower than that with $J = 1$, it can achieve better performance than that with $J = 1$ if the running time is long enough, i.e., longer than 55 s. For those SUs equipped with powerful CPU and large capacity of battery, it is better to set $J = 2$ or even larger. The finally obtained pilot patterns $\boldsymbol{p}$ with the corresponding objective $g(\boldsymbol{p}, \boldsymbol{v})$ during 342 s of running time assuming equal pilot power are listed in Table I. Note that in [14], we suppose $v_1 = v_2 = \cdots = v_{16} = 1$, whereas in this paper, we suppose $v_1 = v_2 = \cdots = v_{16} = 0.0625$ satisfying $\sum_{i=1}^{16} v_i = 1$, the objective in [14] has to be divided by $K = 16$ when compared with this work.

TABLE I
Comparisons of Pilot Patterns Using Different Algorithms or Parameters

Type	$g(\boldsymbol{p}, \boldsymbol{v})$	$\boldsymbol{p}$
CE method	0.3260	47, 95, 110, 162, 180, 193, 246, 513 524, 627, 640, 897, 910, 939, 976, 1019
Algorithm 1 with J = 1, equal	0.3141	18, 45, 57, 103, 141, 187, 242, 256 513, 593, 609, 640, 897, 909, 926, 977
Algorithm 1 with J = 2, equal	0.3077	30, 46, 77, 121, 182, 228, 247, 256 513, 529, 619, 633, 905, 932, 960, 1021
Algorithm 1 with J = 1, joint	0.2945	1,34, 47, 98, 109, 181, 221, 236 252, 513, 529, 609, 635, 900, 934, 959

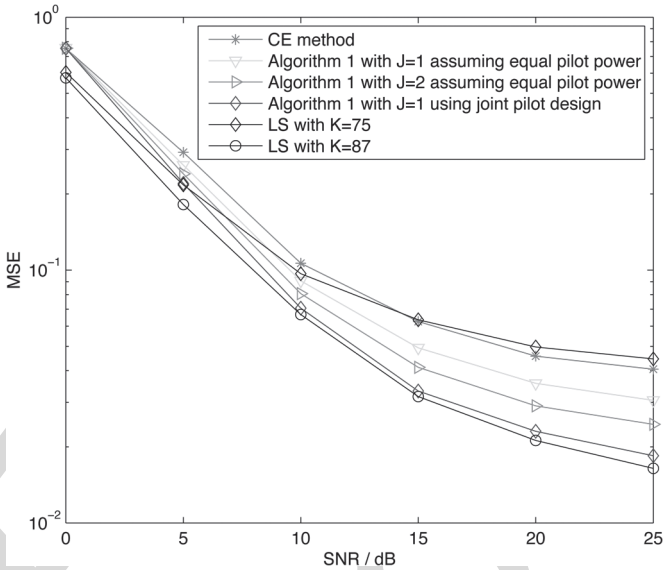

Fig. 3. Comparisons of MSE performance for different algorithms parameters.

We now evaluate the performance of joint design of pilot power and pilot pattern and compare it with the pilot design assuming equal pilot power. As shown in Fig. 2, Algorithm 1 with $J = 1$ using joint pilot design achieves better performance than Algorithm 1 with $J = 1$ or $J = 2$, while its computational complexity is between $J = 1$ and $J = 2$. The obtained pilot pattern with the corresponding objective is also listed in Table I. The comparisons of MSE performance and the bit error rate (BER) performance for sparse channel estimation are shown in Figs. 3 and 4, respectively. Both the MSE and BER are averaged

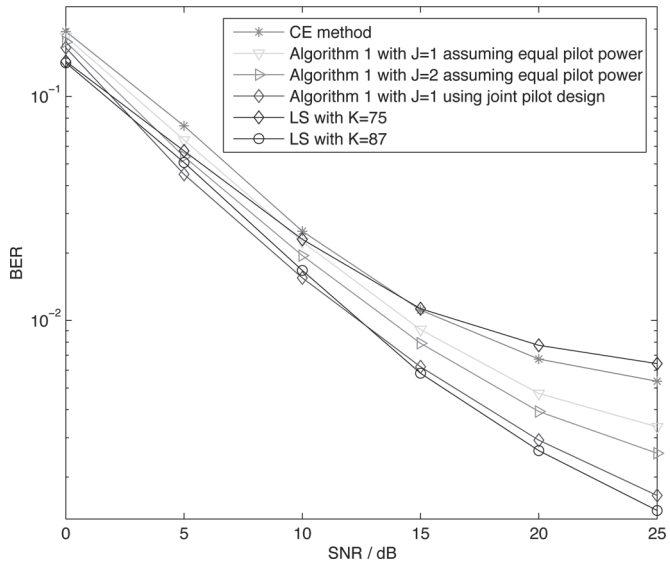

Fig. 4. Comparisons of BER performance for different algorithms or parameters.

over 10 000 sparse channel realizations. The popular OMP algorithm is employed for sparse channel estimation given the designed pilot pattern and pilot power. For comparisons, the performance of LS channel estimation using $K = 75$ and $K = 87$ equally spaced pilots with the pilot interval being 7 and 6, respectively, is also provided. It is seen that Algorithm 1 with $J = 1$ using joint pilot design achieves almost the same performance as LS with $K = 87$. Therefore, the joint design can reduce the pilot overhead by 71 pilots and improve the spectrum efficiency by 13.9%, thus leading to additional 2.4% improvement compared with the pilot design assuming equal pilot power in [14].

VI. Conclusion

In this correspondence, we have investigated the joint design of pilot power and pilot pattern based on the rule of MIP. The pilot design has been formulated as a joint optimization problem, which is then decoupled into tractable sequential formations. Given a pilot pattern, we have formulated the design of pilot power as an SOCP problem. Then, we have proposed a joint design algorithm. Simulation results have verified the effectiveness of the proposed algorithm and shown that the proposed algorithm can achieve better channel estimation performance and further improve the spectrum efficiency by 2.4%, compared with existing algorithms assuming equal pilot power.

References

[1] X. Kang, Y.-C. Liang, A. Nallanathan, H. K. Garg, and R. Zhang, "Optimal power allocation for fading channels in cognitive radio networks: Ergodic capacity and outage capacity," *IEEE Trans. Wireless Commun.*, vol. 8, no. 2, pp. 940–950, Feb. 2009.

[2] Y. Liang, K. C. Chen, G. Y. Li, and P. Mahonen, "Cognitive radio networking and communications: An overview," *IEEE Trans. Veh. Technol.*, vol. 60, no. 7, pp. 3386–3407, Sep. 2011.

[3] D. Hu, L. He, and X. Wang, "An efficient pilot design method for OFDM-based cognitive radio systems," *IEEE Trans. Wireless Commun.*, vol. 10, no. 4, pp. 1252–1259, Apr. 2011.

[4] E. Manasseh, S. Ohno, and M. Nakamoto, "Pilot symbol assisted channel estimation for OFDM-based cognitive radio systems," *EURASIP J. Adv. Signal Process.*, vol. 51, no. 1, pp. 51:1–51:11, Mar. 2013.

[5] J. C. Chen and C. K. Wen, "A novel cognitive radio adaptation for wireless multicarrier systems," *IEEE Commun. Lett.*, vol. 14, no. 7, pp. 629–631, Jul. 2010.

[6] C. R. Berger, Z. Wang, J. Huang, and S. Zhou, "Application of compressive sensing to sparse channel estimation," *IEEE Commun. Mag.*, vol. 48, no. 11, pp. 164–174, Nov. 2010.

[7] C. Qi and L. Wu, "Uplink channel estimation for massive MIMO systems exploring joint channel sparsity," *Electron. Lett.*, vol. 50, no. 23, pp. 1770–1772, Nov. 2014.

[8] P. Pakrooh, A. Amini, and F. Marvasti, "OFDM pilot allocation for sparse channel estimation," *EURASIP J. Adv. Signal Process.*, vol. 59, no. 1, pp. 59:1–59:9, Mar. 2012.

[9] C. Qi and L. Wu, "A study of deterministic pilot allocation for sparse channel estimation in OFDM systems," *IEEE Commun. Lett.*, vol. 16, no. 5, pp. 742–744, May 2012.

[10] J.-C. Chen, C.-K. Wen, and P. Ting, "An efficient pilot design scheme for sparse channel estimation in OFDM systems," *IEEE Commun. Lett.*, vol. 17, no. 7, pp. 1352–1355, Jul. 2013.

[11] C. Qi and L. Wu, "Optimized pilot placement for sparse channel estimation in OFDM systems," *IEEE Signal Process. Lett.*, vol. 18, no. 12, pp. 749–752, Dec. 2011.

[12] X. He, R. Song, and W.-P. Zhu, "Pilot allocation for sparse channel estimation in MIMO-OFDM systems," *IEEE Trans. Circuits Syst. II, Exp. Briefs*, vol. 60, no. 9, pp. 612–616, Sep. 2013.

[13] P. Cheng *et al.*, "Sparse channel estimation for OFDM transmission over two-way relay networks," in *Proc. IEEE ICC*, Ottawa, ON, Canada, Jun. 2012, pp. 3948–3953.

[14] C. Qi, G. Yue, L. Wu, and A. Nallanathan, "Pilot design for sparse channel estimation in OFDM-based cognitive radio systems," *IEEE Trans. Veh. Technol.*, vol. 63, no. 2, pp. 982–987, Feb. 2014.

[15] W. U. Bajwa, J. Haupt, A. M. Sayeed, and R. Nowak, "Compressed channel sensing: A new approach to estimating sparse multipath channels," *Proc. IEEE*, vol. 98, no. 6, pp. 1058–1076, Jun. 2010.

[16] D. Hu, X. Wang, and L. He, "A new sparse channel estimation and tracking method for time-varying OFDM systems," *IEEE Trans. Veh. Technol.*, vol. 62, no. 9, pp. 4648–4653, Nov. 2013.

[17] E. J. Candes and T. Tao, "Decoding by linear programming," *IEEE Trans. Inf. Theory*, vol. 51, no. 12, pp. 4203–4215, Dec. 2005.

[18] T. Cai and L. Wang, "Orthogonal matching pursuit for sparse signal recovery with noise," *IEEE Trans. Inf. Theory*, vol. 57, no. 7, pp. 4680–4688, Jul. 2011.

[19] M.-S. Lobo, L. Vandenberghe, S. Boyd, and H. Lebret, "Applications of second-order cone programming," *Linear Algebra Appl.*, vol. 284, no. 1–3, pp. 193–228, Nov. 1998.

AUTHOR QUERY

NO QUERY.